Modelling and Performance Evaluation of a Photovoltaic/thermal Solar Energy System in Oman Using Experimental Data and Artificial Neural Networks

Asil M. K. Al Khaldi
Faculty of Engineering, Sohar University

Al-Ghaliya A. S. Al-Marzouqi
Faculty of Engineering, Sohar University

Hussein A. Kazem
Faculty of Engineering, Sohar University

Miqdam T. Chaichan
Energy and Renewable Energies Technology Research Centre, University of Technology

https://doi.org/10.5109/7342473

出版情報：Evergreen. 12 (1), pp.541-552, 2025-03. Interdisciplinary Graduate School of Engineering Sciences, Kyushu University, Japan
バージョン：

Modelling and Performance Evaluation of a Photovoltaic/thermal Solar Energy System in Oman Using Experimental Data and Artificial Neural Networks

Asil M. K. Al Khaldi[1], Al-Ghaliya A. S. Al-Marzouqi[1], Hussein A. Kazem[1,*], Miqdam T. Chaichan[2]

[1]Faculty of Engineering, Sohar University, 3111 Al Jamiah Street, Sohar 311, Oman

[2]Energy and Renewable Energies Technology Research Centre, University of Technology, Al Senaha St, Baghdad, Baghdad Governorate, Iraq

*Author to whom correspondence should be addressed:
E-mail: h.kazem@soharuni.edu.om

(Received August 28, 2024; Revised January 24, 2025; Accepted February 19, 2025).

Abstract: Photovoltaic thermal (PV/T) hybrid systems harness solar energy by simultaneously generating heat and electricity from sunlight. These systems consist of metallic panels with solar cells covered by glass, designed to convert sunlight into energy while absorbing heat. The research in this field has focused on improving PV/T efficiency, particularly in managing the heat that can negatively impact PV cell performance. This study explores the effects of temperature on the power, voltage, current, and thermal and electrical efficiencies of PV/T systems, aiming to enhance PV efficiency through experimental research.

Focusing on Oman's weather conditions, the study demonstrates that integrating thermal components significantly improves solar energy system performance, increasing the maximum output power of the PV system from 10.302 W to 11.607 W. Using empirical data, an artificial neural network model was developed with the multilayer perceptron approach, achieving high predictive accuracy. The analysis revealed minimal mean squared error values of 0.0055 for the PV system and 0.1358 for the PV/T system, along with a high coefficient of determination (R value) of 1 for the PV system and 0.9995 for the PV/T system. This study highlights the effectiveness of thermal component integration in enhancing solar energy system efficiency in Oman.

Keywords: Photovoltaic/thermal; solar energy; ANN; MLP

1. Introduction

Photovoltaic thermal (PV/T) integration refers to systems whereby photovoltaic (PV) cells are combined with thermal collectors. These systems also produce electrical energy as well as store heat energy from the sun[1)]. In a normal sense, the initial sector of the PV/T system is the photovoltaic cells which convert the sun rays into electricity. Nonetheless, individual PV cells are capable of converting only a certain portion of the received solar energy, and the rest of the energy is mostly converted into heat[2,3)]. In a PV/T system, this excess heat is picked up by a thermal collector which normally uses a fluid such as water or air, which flows beneath or around the PV cells[4)]. It can be used for heating as in water heating space heating or even cooling depending on the design of the system[5,6)].

Even with the similarities of both kinds of systems, the use of PV/T can generate both electrical and thermal energy with better efficiencies than either PV or solar thermal systems. Mainly they are useful in situations where both electric power and heat are essential, like in households and offices, industries, and farming[7)]. PV/T systems combine two collectors to boost efficiency, lower costs, and take up less space while simultaneously generating energy and heat as shown in Fig. 1. The generation of PV/T current, voltage, power, efficiency, and heat energy is influenced by numerous variables. Such parameters include the PV system's location, ambient temperature, irradiance, humidity, dust, and many others[8,9)]. Additionally, several modelling methodologies, such as analytical, regression, numerical, and artificial neural network (ANN), are utilized to assess PV/T efficiency[10,11)].

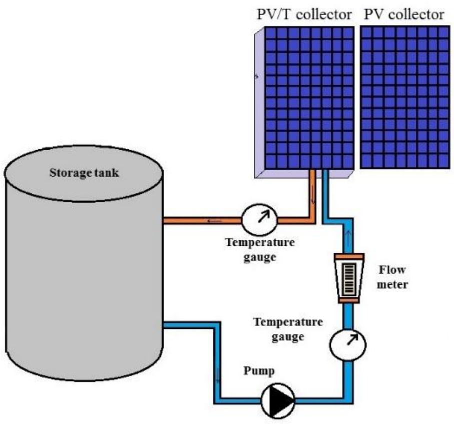

Fig. 1: PV/T system.

Several studies were conducted to model and investigate PV/T systems. Table 1 presents a comprehensive comparison spanning the years 2011 to 2023, incorporating diverse geographical locations worldwide. This comparative analysis is cantered on modelling and predicting PV/T performance, providing a systematic breakdown of key criteria.

Table 1. Comparison of PV/T performance modelling using ANN.

Reference	location	Year	ANN model	Input parameters	Findings
3)	Oman Sohar 24.3461N 56.7075E	2021	MLP (3 layers) SOFM SVM	G, T_a	MSE= 0.04457 NMSE= 0.26399 MAE= 0.65084 Min Abs Error= 0.01337 R= 0.85800
4)	India	2023	MLP	G, T_a, RH, WS, T_i, T_o	η_{th} = 50.7% η_{elec} = 12.15% R= 0.99843 MSE=0.03134
5)	Malaysia Bangui 18.558N 4.395E	2019	MLP	G, T_a	R^2= 0.81 RMSE= 0.371 MSE= 0.036
7)	Iran Ahrood 34.64N 50.876E	2019	MLP	G, T_a, FR	R^2= 1 MSE= 0.093
8)	Mexico Yucatan city -89.094N 20.709E	2017	ANFIS	RH, T_a, WE	R^2= 0.81 RMSE= 0.371 MSE= 0.036
9)	Iran Kermanshah 34.457N 46.670E	2019	PSO	L, D, W, T_a	R^2= 0.998 MAE= 3.63 MSE= 0.026
11)	Oman Sohar city 24.3461N 56.7075E	2017	MLP PSO	G, T_a, RH	R^2= 0.998 MAE= 3.6 MSE= 0.03
12)	India Kalyani city 22.9751N 88.4345E	2017	Deep Learning DL	SH, T_i, T_o	MSE= 0.0043 MAE = 1.7855
13)	Oman Sohar city	2017	MLP GFF	G, T_a	MSE = 0.06543 RMSE = 0.2539

	24.3461N 56.7075E		SOFM		MAPE = 5.718 NMSE = 0.2355 MAE = 7.2593 R^2 = 0.9109
14)	Oman Sohar 24.3461N 56.7075E	2024	SOFM MLP	G, RH, T_a	MSE = 0.001 MAE = 36.1% R^2 = 0.999
15)	Turkish Osmaniye 37.05N 36.14E	2017	ANN	G, RH, WS, T_a	RMSE = 0.398 MAPE = 11.668 MAE = 0.456 R^2 = 0.868
16)	Iran 32.1648N 48.25E	2011	MLP	RH, T_a, EV, SH, WS	MAPE= 6.08% R^2= 0.9904 MSE= 0.0042
17)	UAE Al-Ain 24.1302N 55.8023E	2011	MLP RBF	RH, T_a, SH, WS	RMSE= 0.349 R^2= 0.92 MAE= -0.571

Note: RH is relative humidity, T_a is ambient temperature, EV is Evaporation, SH is sunshine hours, WS is wind speed, G is Solar irradiance, FR is flowrate, L is length, D is depth, W is width, T_i is intel temperature, T_o is outlet temperature, η_{th} is thermal efficiency, η_{elec} is electrical efficiency

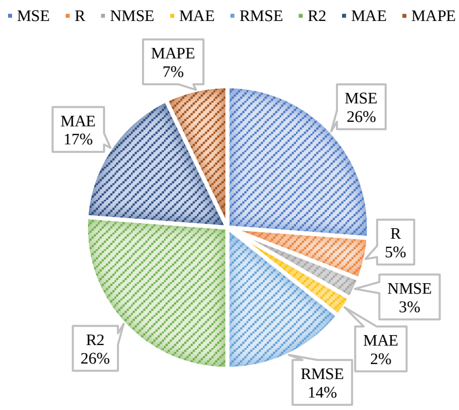

Fig. 2: Comparison of PV/T modelling evaluation criteria.

The provided data in Fig. 2 illustrates the frequency of various modelling evaluation criteria employed in research studies which are R^2, MSE, R, RMSE, MBE, MAE, NMSE, and MAPE. Particularly, "Mean Squared Error" (MSE) and "Coefficient of Determination" (R^2) are the most frequently utilized criteria. This prevalence highlights the significance of MSE and R^2 in evaluating the performance and accuracy of predictive models, particularly in the context of modelling PV/T systems. Extensive literature supports the selection of these parameters as they are widely regarded as robust indicators of predictive accuracy and performance consistency. For instance, MSE effectively quantifies the average squared error, emphasizing large deviations, while R^2 evaluates the proportion of variance explained by the model. Studies such as [insert key references here] have consistently demonstrated their reliability and applicability in solar energy research, particularly for PV/T systems.

The choice of MSE and R^2 in the current study is informed by a thorough examination and comparison of multiple studies, underscoring their reliability and relevance as essential metrics for assessing the success of predictive models. Moreover, their use aligns with established research practices, ensuring consistency and comparability of results within the domain of solar energy research.

Figure 3 presents MSE values from various research studies conducted between 2011 and 2023, offering insights into the predictive accuracy of different models. Especially, References[3] and[12], which stand out with the minimum MSE of 0.004, suggesting a high level of precision in its predictions. The authors use G, RH, T_a, EV, SH, and WE as input parameters. This research merits attention for its exceptional performance in minimizing prediction errors on the other end of the spectrum.

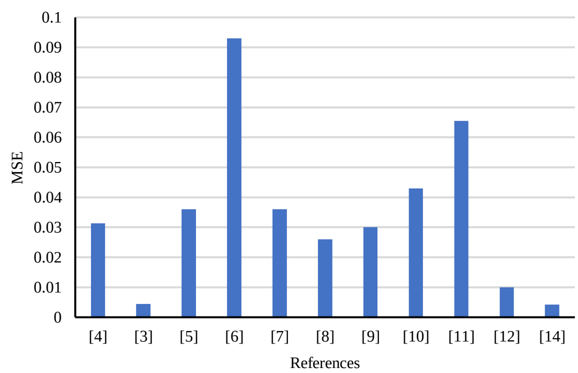

Fig. 3: Comparison PV/T modelling MSE.

Reference[7] demonstrates the maximum MSE of 0.093, signifying a relatively higher level of discrepancy between predicted and actual values. The considerable MSE[6] may indicate potential limitations or challenges in the predictive model employed. The used input parameters were G, T_a, and FR.

Figure 4 presents R^2 values from diverse research studies conducted between 2011 and 2023, offering insights into the goodness of fit of various predictive models. Especially[7,8,10,14], and[16] emerge with the highest R^2 values approximately 0.999, indicating a remarkably close alignment between predicted and actual values and demonstrating high accuracy and reliability in their modelling approaches.

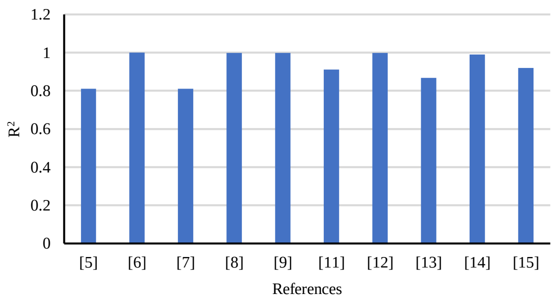

Fig. 4: Comparison PV/T modelling R^2.

Conversely,[5] and[8] exhibit R^2 values of approximately 0.800, implying a comparatively lower level of precision in their predictions than observed in other studies. It is crucial to note that R^2 values closer to 1 signify a better fit, while values closer to 0 indicate weaker model performance. These findings emphasize the importance of scrutinizing R^2 values in solar energy research, providing valuable insights into the effectiveness of various predictive models for PV/T.

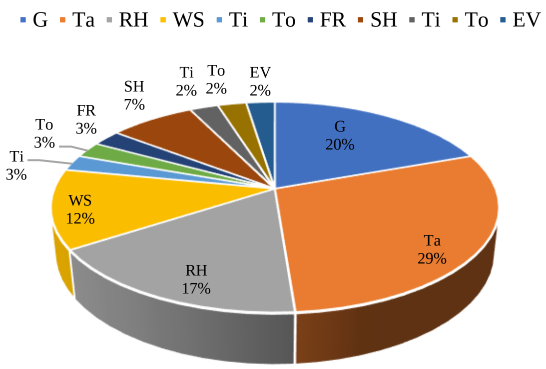

Fig. 5: Comparison of PV/T modelling input parameters.

The data in Fig. 5 explains the frequency of distinct input parameters in various research studies, with ambient temperature and solar irradiance emerging as the most recurrently employed input variables. The consistent utilization of T_a and G highlights their paramount significance in the modelling and prediction of PV/T systems. The two mentioned parameters will be used in this study.

The review of used ANN methods in Fig. 6 across research studies reveals that the MLP is the most frequently employed method. This widespread usage highlights MLP's effectiveness. In this study, MLP was used to model the PV/T system. MLP's demonstrated success, reflecting its robustness and suitability for capturing the intricate relationships within PV/T systems.

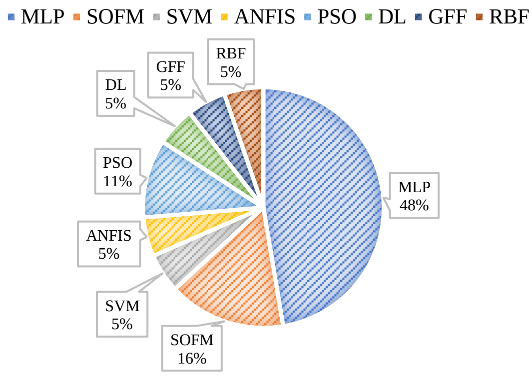

Fig. 6: Comparison of PV/T ANN modelling methods.

Aligning with established practices, using MLP ensures a reliable and consistent modelling approach based on insights gained from an extensive literature review and method comparison[17,18].

Reference[19] studied the feasibility of measuring the performance of a flat solar collector using an intelligent neural network model. The researchers conducted several experiments in multiple arrangements (discrete, serial, and parallel). The experimental results were used to build a generalized regression neural network model design. The proposed model has mass flow rate, solar radiation, fluid temperature difference, and collector area as inputs while its outputs were power output and efficiency. The final accuracy of the developed model was about 98%.

The usage of conventional energy sources in Oman affects the environment and considerably increases GHG emissions. With Oman's environment being marked by a lot of sunshine all year long, there is a special chance to use solar energy as a sustainable substitute. Many challenges faced in this issue included the ability to design, simulate, and shift PV/T solar energy systems that will be reliable, efficient, and optimized for the Oman climate conditions. The following are the challenges encountered while designing, simulating, and implementing PV/T solar energy systems:

The first problem of focus is the absence of a perfect and efficient system of PV/T in Oman that will effectively harvest and convert solar radiation to useful heat energy. It is envisaged that such a system should be structurally planned and modelled maximally to ensure high energy efficiency given the local climatic factors such as heat, high humidity, and dust storms. The system should also be evaluated based on the results, including the effectiveness, cost, and time effectiveness of the system, and the effective use of natural resources.

By addressing this problem, one can work with Oman's solar power potential, leading to tremendous energy conservation and a lesser demand for standard hydrocarbons[20]. The significance of this research lies in the optimization of efficiency, reduction of cost and space, and the combined production of heat and electricity. This current study employs the ANN modelling methodology that operates with the help of an experimental dataset of Oman to foresee and assess a PV/T system.

Hence, the proposed study that aims at planning, simulating, and analyzing an Oman-based PV/T system will contribute to the development of the literature in the field of renewable energy. The research will be using experimental findings and ANN to make the performance and effectiveness of the system better. The objective of the present study is threefold: (i) to propose a PV/T system relevant to Oman's climate and energy demand, (ii) to investigate experimentally the behavior of the surfaced developed design in outdoor conditions and (iii) to employ ANN method for modelling and predicting the performance of the PV/T system.

2. Methodology

For the coding and analysis of this PV/T system's performance and output simulation in Oman, MATLAB was used. The gathered data was used for training, cross-validation, and testing as depicted in Fig. 7 above. In the same respect, cross-validation data was used for adjusting the model weights whilst test data for evaluating the performance of the proposed PV/T model. The training was to be done to a maximum of 1000 iterations to allow a thorough training of the network. The inputs of the model consisted of ambient temperature and the radiation from the sun while the output comprised the current and voltage of the PV/T system.

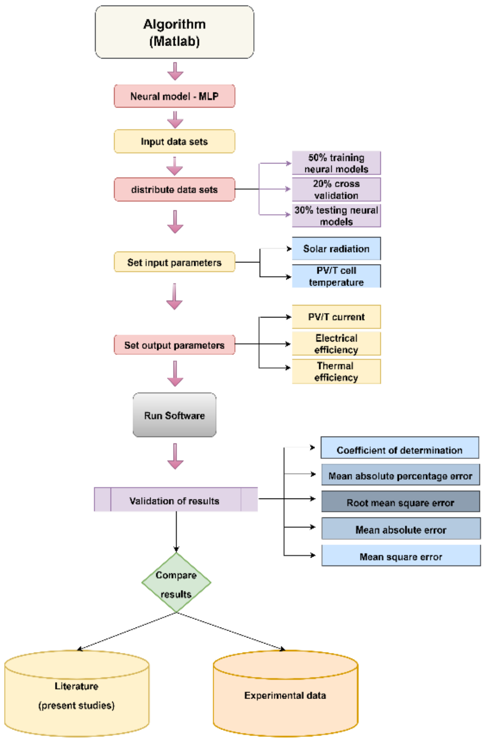

Fig. 7: Research methodology.

2.1 System description

As concerns the construction of the PV/T module and the flow of water through it to absorb thermal heat, an overview is shown in Fig. 8 (a). The developed module comprises four anti-of-anti layers. The finishing layer is a glass plate – this layer serves not only as a material top layer but also as an anti-reflective cover due to the special coating. Below that a PV/T module can be seen which is made of Ethylene Vinyl Acetate (EVA) layer and a Tedlar Polyester Tedlar (TPT) layer. It has some important functions of safeguarding the photovoltaic cells against water penetration and subsequent damage which hinders the sturdiness and competence of the module.

These water pipes, which work as thermoclines are mounted at the backside of the module as can be seen in the figure below. These pipes consist of a folded copper pipe that is tightly fixed and is intended to absorb heat from the panel. More details of this setup are described in Fig. 8(b) in which the process of heat transfer has been illustrated. The last layer of the regard module is graphite, which improves the thermal conductivity of this layer and, therefore, increases the heat exchange in the system.

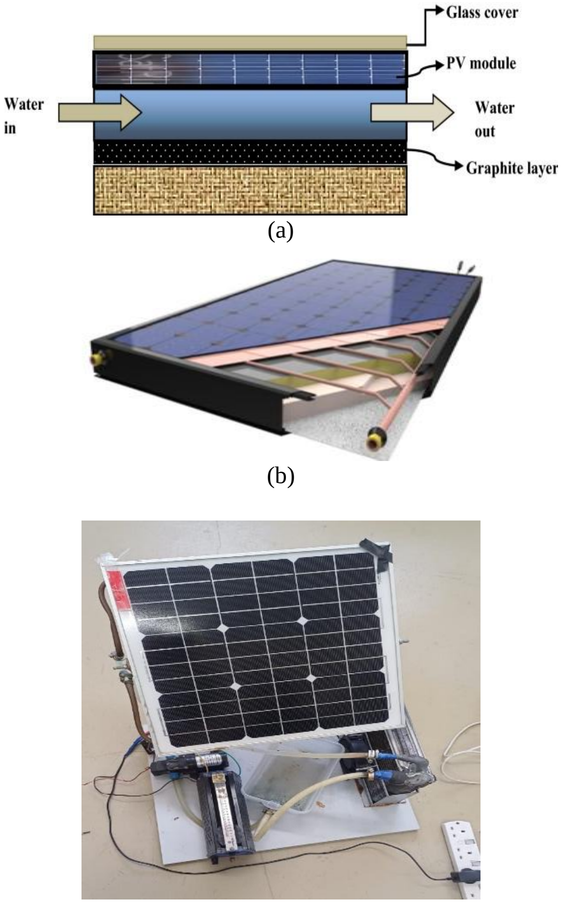

(a)

(b)

(c)

Fig. 8: (a) component of the PV/T module (b) the pipe collects the heat (c) experimental rig.

The major parts of the PV/T system are a photovoltaic (PV) module, a water pump, thermal collector – pipes and a radiator, a DC fan, and electric/metal-thermal sensors. The PV module has a power rating of 20W, Isc of 1. 27A, and an open-circuit voltage (Voc) of 21. 9V. The DC water pump, which is used to circulate the coolant works at the maximum output of 45W, and the maximum pressure produced is 0.75 Mpa. The thermal collector comprises pipes for heat collection and heat transfer. The radiator and the DC fan are employed to cool down and prevent overheating of the circuits. The system has electrical and thermal sensors that give accurate data on the performance of the power system. In the real system configuration, the components in the PV/T system can be set up as shown in Fig. 8(c). Table 2 lists the used measuring devices and their uncertainties.

Table 2. used measuring devices uncertainties.

Equipment	Measured Parameter	Experimental uncertainty (%)
Solar radiation intensity meter	Irradiance	±1.2
Thermocouples	Temperature (PV module, PV/T collector, inlet, outlet, and ambient)	±0.19
Flow meter	Coolants' flow rate (kg/s)	±0.22
Multi-meter	Voltage	±0.05
Multi-meter	Current	±0.03

2.2 Local climate

Irradiances and ambient temperatures recorded in Sohar, Oman have been plotted in Fig. 9 and these records provide a record of the solar irradiance during the daytime in the region. The baseline solar irradiance entering the Earth's atmosphere approximately is 1000 W/m². The February measurements reflect the actual solar irradiance levels received on the ground, providing a detailed understanding of the local solar conditions.

The dataset, measured using a Pyranometer, reveals that irradiance values vary throughout the day. The readings begin at 371.0 W/m² and gradually increase, peaking at 644.7 W/m² before slowly declining. Particularly, solar irradiance increases steadily until around noon (12:05), after which it begins to decrease. These fluctuations in radiation are influenced by factors such as atmospheric conditions, cloud cover, and the Earth's tilt, all of which affect the surface's direct exposure to sunlight. The daily radiation curve exhibits a distinct pattern. The peak value of 644.7 W/m² represents the highest solar irradiance, typically occurring around solar noon, while the minimum value of 264.2 W/m² corresponds to the lowest irradiance levels, usually observed in the early morning or late afternoon. The average daily irradiance was calculated to be 496.89 W/m², offering a comprehensive overview of the solar energy available in the region throughout the day.

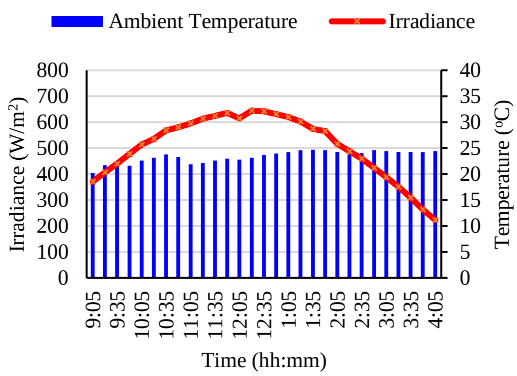

Fig. 9: Irradiance and ambient temperature in sohar.

2.3 Test Procedure

In this study, the performance and efficiency of a PV/T system cooled with water and air were studied. The PV system was designed, installed, and measured in real time outside the laboratory. The tested systems:

• Conventional solar cells (PV), which were considered the main reference.

• A combined water and air-cooled PV system.

The first experiments were conducted on sunny and clear days, and during these experiments, the solar radiation intensity was measured instantly. Starting from June 3, 2017. The measurements were started at 8 am and ended at sunset. The water inlet and outlet were measured every half an hour as well as the ambient temperature. The water pumps and fan continued to operate after sunset to cool the PV module and continued to operate until it was confirmed that the panel's temperature was equal to the ambient air temperature to be ready for the next day's experiments.

2.4 ANN modelling

MLP is a feed-forward neural network, meaning that information travels in one direction—from the input layer through hidden layers to the output layer—without forming cycles or loops[21]. In MLP, connections between nodes are assigned weights adjusted during training to minimize the difference between predicted and actual outputs[22,23]. The backpropagation algorithm is commonly used for this purpose, propagating errors backward through the network to update weights. Activation functions in the hidden layers introduce non-linearity, facilitating the learning of intricate data relationships. Sigmoid, hyperbolic tangent (tanh), and rectified linear unit (ReLU) are among the commonly used activation functions. These components collectively enable MLPs to effectively learn and model complex patterns in various types of data.

The backpropagation learning method calculates network errors and enables weight adjustments for the hidden layers. Which is defined in equation (1)[24,25]:

$$e_i(n) = d_i(n) - y_i(n) \quad (1)$$

where d_i is the desired dataset, and y_i is the computed data value

A delayed convergence is caused by the cost function gradient's slow evolution between iterations. To solve this issue and accelerate convergence, the momentum learning technique is applied, which will smooth the behavior. Equation (2) is used to calculate the momentum learning method[26].

$$w_{ij}(n + 1) = w_{ij}(n) + \eta\delta_i(n) + x_j(n) + \alpha\,(\,w_{ij}(n) - w_{ij}(n - 1)\,) \quad (2)$$

α is the momentum factor, set to 0.7, η is the constant step size, δ_i(n) is the local error.

ANNs are evaluated using various metrics, including MSE, R, R^2, MAPE, RMSE, and COV. MSE is a critical metric representing the average of squared prediction errors[27,28]. It quantifies prediction accuracy and is calculated as the second moment of the error from the origin, as per equation (3)[29].

$$MSE = \frac{1}{n}\sum_{i=1}^{n}(\,Y_i - X_i)^2 \quad (3)$$

where Y_i is the n number of predictions, X_i is the n number of true values.

R^2 is a statistic that ranges from 0% to 100% that shows how near the data are to the fitted regression line. A value of zero signifies that none of the data's variables are centered around the mean, whereas a value of 100 implies that every variable is[30],

$$R^2 = 1 - \frac{SSE}{SST} \quad (4)$$

3. Results and discussion

3.1 Experimental results

Figure 10 represents the relationship between the T_a and time. T_{in} and T_{out} denote the temperatures of the water employed to cool the module at the entry and exit points, respectively. It's seen that there is no relation between T_a and the temperature of the water in the PV/T system. However, T_{in} is lower compared with T_{out}, which means that the heat is transferred from the PV module to the water through the collector pipes[31].

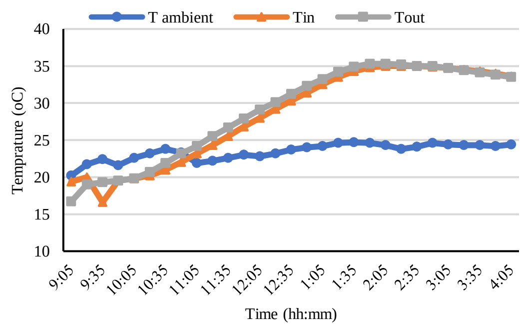

Fig. 10: T_a, T_{in}, and T_{out} the PV/T system.

The plotted values in Fig. 11 depict the voltage of both PV and PV/T systems, measured at 15-minute intervals from 9:05 AM to 4:05 PM. Initially, the voltage is notably low as sunlight hasn't fully struck the cells to generate optimal voltage. As the graph progresses, it becomes evident that PV/T consistently records higher voltage compared to PV.

The maximum measured voltage for PV/T is 21.9 V, surpassing the 20.2 V attained by the PV system. This difference highlights the positive impact of the cooling system on performance. This result is consistent with the results of references[31] and[32].

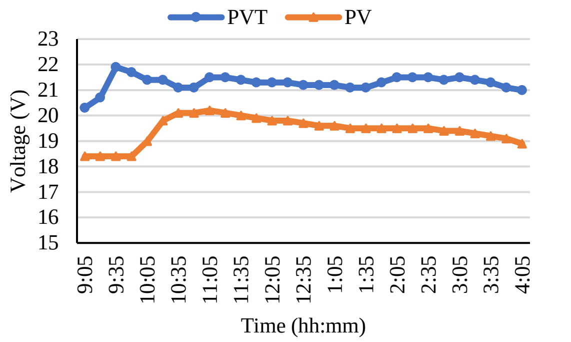

Fig. 11: Comparison between the PV and PV/T voltages.

Figure 12 shows a comparison between the PV and PV/T output powers, which reveals notable differences in the power generated by each system. Comparing the maximum power outputs of the PV/T and PV reveals that the PV/T system attained a higher peak power of 11.607 W while the conventional PV system reached a maximum of 10.302 W. This observation suggests that the incorporation of a thermal component in the PV/T system contributes to enhancing power generation, potentially due to better temperature regulation and improved overall efficiency. References[33] and[34] have concluded a similar result.

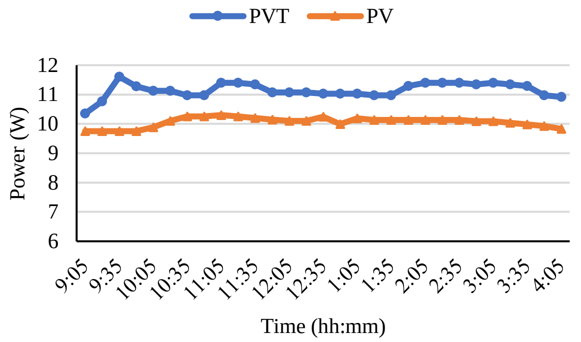

Fig. 12: Comparison between the PV and the PV/T output currents.

3.2 ANN results

The experimental data obtained from PV and PV/T systems serves as input for ANN prediction, facilitated through the implementation of the MATLAB neural network time series model known as Nonlinear Autoregressive with External input (NARX). An architecture and visual representation of this proposed model is depicted in the accompanying chart in Fig. 13.

The training and testing of the MLP network involve dividing the dataset into three parts: 70% for training, 15% for testing, and 15% for validation. The network undergoes multiple training iterations to optimize the MSE and R^2 for prediction error and accuracy. The training and testing involve specifying input variables like G and T_a. In a PV system without thermal components, power, current, and voltage are the outputs, whereas in a PV/T system, besides electrical components there is T_{in} and T_{out} serve as outputs.

The 'nntool' function is utilized for designing the ANN MLP model and for training and testing purposes. Normalization of the target using the "mapstd" function ensures a mean of zero and unity deviation, followed by assessing the error.

The predictive validity is evaluated using the R^2 by comparing the results with those obtained from the real model. Additionally, MSE is calculated to validate the predicted results further.

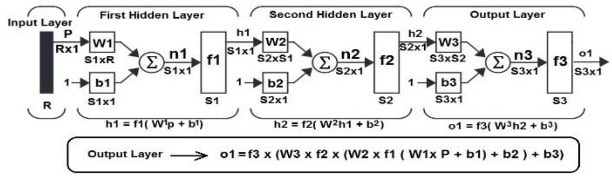

(a)

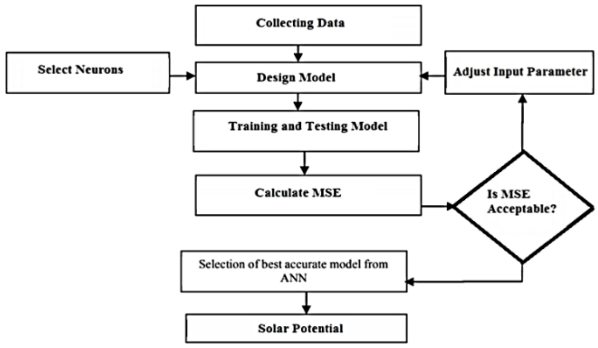

(b)

Fig. 13: ANN (a) architecture, (b) implementation method.

Figure 14(a) and (b) depict the regression analysis of thermal collector and non-thermal panels, showing R^2 of 0.99883 and 0.99991, respectively. In addition, MSE was found to be 0.0055,

which is very low in comparison with other models in the literature illustrated in Table 1. These figures demonstrate the distribution of targets across training, validation, and test sets, with the optimal fit lying along the 45-degree line where outputs match targets. Particularly, the PV/T system data exhibits a strong alignment. Analysis using neural networks reveals that the MLP model surpasses traditional statistical methods, closely resembling measured values. This emphasizes the effectiveness of neural networks in predicting energy for PV/T system performance[34].

Figure 15 (a) and (b) serve as graphical representations showcasing the predictive output values (power and voltage) generated by the ANN model for the PV and PV/T systems and compare results with the experimental values. These figures offer insight into the model's predictive capabilities, shedding light on its performance under varying conditions and system configurations by using the ANN model. The figures indicate that the power and voltage generated by the PV system with thermal components are higher than those without thermal parts.

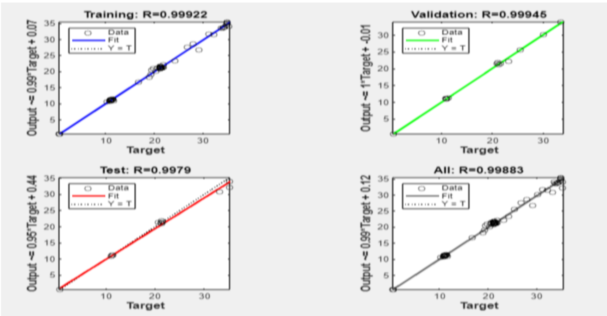

(a)

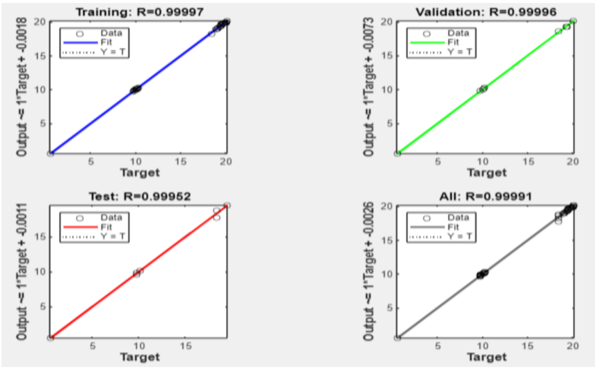

(b)

Fig. 14: Regressions for (a) PV, (b) PV/T.

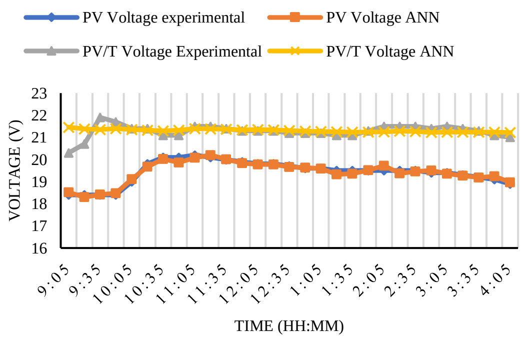

(a)

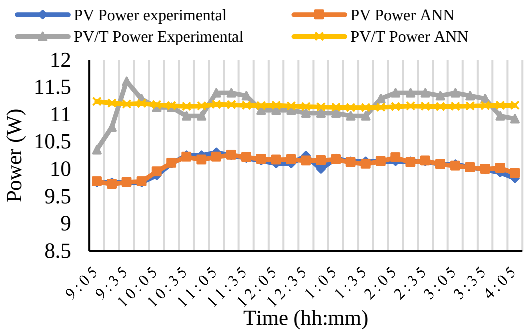

(b)

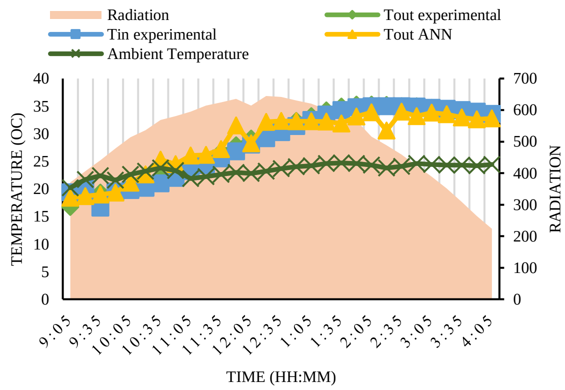

(c)

Fig. 15: Comparing PV and PV/T performance for the predictive and experimental results.

Moreover, the predictive power and voltage closely approximates the experimental power for both the PV and PV/T systems. While there is a slight difference between the PV and PV/T systems output current even by experiment or ANN prediction. References[35,36] and[37] gave similar results to these.

4. Conclusion

In the present work, a new PV/T system was created and simulated to fulfill the climatic and energy requirements of Oman. Local climatic conditions were used to gauge the efficiency of the systems, thus testing the feasibility of the system operationally. The practical results indicated that the outpower of the PV/T system was increased by 12.66 compared to PV module ones.

And so, from the experimental data and sophisticated ANN simulations, it was revealed that the system behaves and can be modelled in a like manner. The implementation of the ANN models concerning the MLP approach also enabled the accurate evaluation of the weather conditions and possibilities of energy generation in the Sohar region in Oman. The model shows great predictive accuracy proving the lowest possible MSE of 0. 0055 for the PV system and 0. 955 for the PV/T system while a near-perfect coefficient of determination R2 = 1 was determined for the PV system and 0.9995 for the PV/T system. Thus, enhancing thermal components in solar power systems is a vital strategy for improving the efficiency of such systems in the region.

Furthermore, comparative analysis is done to assess the potential efficiency of the optimized model in terms of the electrical and thermal performance of both PV and PV/T systems. This analysis therefore provides a solid framework within which decision-makers can accurately predict future energy needs and determine the potential of renewably generated energy in Oman as well as deliberate and decide on the likely feasibility of the implementation of renewable energy technologies. Therefore, the outcomes of the study enhance the overall knowledge about the application of specialized systems in employing solar energy in certain geographic conditions that enable sustainable change toward clean energy.

Nomenclature

ANN	Artificial Neural Network
G	Solar Irradiance
Isc	Short Circuit Current
PV	Photovoltaic
PV/T	Photovoltaic/Thermal
MAE	Mean Absolute Error
MAPE	Mean Absolute Percentage Error
MBE	Mean Bias Error
MSE	Mean Squared Error
MLP	Multilayer Perceptron
NMSE	Normalised Mean Square Error
R	Coefficient of correlation
R^2	Coefficient of Determination
RMSE	Root Mean Squared Error
T_a	Ambient Temperature
T_{in}	Input Temperature
T_{out}	Output Temperature
Voc	Open Circuit Voltage

References

1) H. Madhi, S. Aljabair, A.A. Imran, "A review of photovoltaic/thermal system cooled using mono and hybrid nanofluids," *International Journal of Thermofluids*, 100679 (2024). https://doi.org/10.1016/j.ijft.2024.100679
2) Y.S. Indartono, A.M. Nur, A. Divanto, and A. Adiyani, "Design and testing of thermosiphon passive cooling system to increase efficiency of floating photovoltaic array," *EVERGREEN*, 10 (01) 480-488 (2023). https://doi.org/10.5109/6782151
3) K. Verma, O. Prakash, A.S. Paikra, and P. Tiwari, "Photovoltaic panel integration using phase change material (PCM)," *EVERGREEN*, 10 (01) 444-453, (2023). https://doi.org/10.5109/6782147
4) B.A. Shallal, E. Gidik, H.A. Abdul Wahab, M.G. Ajel, "Impact of alumina nanoparticles additives on open-flow flat collector performance for PV panel thermal control application," *EVERGREEN*, 10(02) 870-879, (2023). https://doi.org/10.5109/6792842
5) A. Beniwal, C. Kumar, D.K. Sharma, and A. Jhalani, A., "Thermal regulation and performance improvement of solar PV panel using PCM OM29." *EVERGREEN*, 10(4) 2583-2589 (2023). https://doi.org/10.5109/7160913
6) A.H. Al-Waeli, H.A. Kazem, M.T. Chaichan, and K. Sopian, "A review of photovoltaic thermal systems: Achievements and applications." *International Journal of Energy Research*, 45(2) 1269-1308 (2021). https://doi.org/10.1002/er.5872
7) J.H. Yousif, and H.A. Kazem, "Prediction and evaluation of photovoltaic-thermal energy systems production using artificial neural network and experimental dataset," *Case Studies in Thermal Engineering*, 27 101297 (2021). https://doi.org/10.1016/j.csite.2021.101297
8) M.J. Deka, P. Kalita, D. Das, A.D. Kamble, B.J. Bora, P. Sharma, and B.J. Medhi, "An approach towards building robust neural networks models using multilayer perceptron through experimentation on different photovoltaic thermal systems," *Energy Conversion and Management*, 292 117395 (2023). https://doi.org/10.1016/j.enconman.2023.117395
9) S.F.Z. Asl, A. Karami, G. Ashari, A. Behrang, A. Assareh, and N. Hedayat, "Daily global solar radiation modeling using multi-layer perceptron (MLP) neural networks." *International Journal of Environmental and Ecological Engineering* 5(7) 403-405 (2011). https://citeseerx.ist.psu.edu/ (Accessed 11 November 2024)
10) M.W. AlShaar, Z. Al-Omari, W. Emar, M. Alnsour, and G. Abu-Rumman, "Application of PV-thermal array for pumping irrigation water as an alternative to PV in Ghor Al-Safi, Jordan: A case study." EVERGREEN, 09(04) 1140-1150 (2022). https://doi.org/10.5109/6625725
11) A.H. Al-Waeli, H. A. Kazem, J.H. Yousif, M.T. Chaichan, and K. Sopian, "Mathematical and neural network models for predicting the electrical performance of a PV/T system," *International Journal of Energy Research*, 43 (14) 8100-8117 (2019). https://doi.org/10.1002/er.4807
12) M. Sridharan, "Application of generalized regression neural network in predicting the performance of solar photovoltaic thermal water collector," *Annals of Data Science*, 10(1) 1-23 (2023). https://doi.org/10.1007/s40745-020-00273-1
13) A.K. Sethi, A.K. Sharma, S. Chandra, and A. Rawat, "The photovoltaic (PV) module performance analysis using artificial neural network (ANN)". *EVERGREEN*, 11 (02) 1273-1278 (2024). https://doi.org/10.5109/7183435
14) M. Zamen, A. Baghban, S.M. Pourkiaei, and M.H. Ahmadi, "Optimization methods using artificial intelligence algorithms to estimate thermal efficiency of PV/T system," *Energy Science & Engineering*, 7 (3) 821-834 (2019). https://doi.org/10.1002/ese3.312
15) A. Bassam, O. May Tzuc, M. Escalante Soberanis, L.J. Ricalde, and B. Cruz, "Temperature estimation for photovoltaic array using an adaptive neuro fuzzy inference system," *Sustainability*, 9 (8) 1399 (2017). https://doi.org/10.3390/su9081399
16) A.A. Alnaqi, H. Moayedi, A. Shahsavar, and T.K. Nguyen, "Prediction of energetic performance of a building integrated photovoltaic/thermal system thorough artificial neural network and hybrid particle swarm optimization models," *Energy conversion and management*, 183 137-148 (2019). https://doi.org/10.1016/j.enconman.2019.01.005

17) J.H. Yousif, H.A. Kazem, and J. Boland, "Predictive models for photovoltaic electricity production in hot weather conditions," *Energies*, 10 (7) 971 (2017). https://doi.org/10.3390/en10070971
18) S. Dey, S. Pratiher, S. Banerjee, and C.K. Mukherjee, "Solarisnet: A deep regression network for solar radiation prediction," arXiv *preprint arXiv:1711.08413* (2017). https://doi.org/10.48550/arXiv.1711.08413
19) M. Sridharan, and S. Shenbagaraj, "Application of generalized regression neural network in predicting the thermal performance of solar flat plate collector systems". *Journal of Thermal Science and Engineering Applications*, 13 (2), 021023 (2021). https://doi.org/10.1115/1.4047824
20) K. Okedu, H. Nadabi, A. Aziz, "Prospects of solar energy in Oman: Case of oil and gas industries." *International Journal of Smart Grid-ijSmartGrid*, 3(3), 138-151 (2019). https://doi.org/10.20508/ijsmartgrid.v3i3.68.g63
21) T.L. Fine, "Feedforward Neural Network Methodology." Springer Science & Business Media, 1999, 1st Edition. https://books.google.com.om/ (Accessed 11 November 2024)
22) A.F. Murray, and P.J. Edwards, "Enhanced MLP performance and fault tolerance resulting from synaptic weight noise during training." *IEEE Transactions on neural networks*, 5(5) 792-802 (1994). https://doi.org/10.1109/72.317730
23) H.A. Kazem, J.H. Yousif, and M.T. Chaichan, "Modeling of daily solar energy system prediction using support vector machine for Oman," *International Journal of Applied Engineering Research*, 11 (20) 10166-10172 (2016). http://www.ripublication.com (Accessed 22 November 2020)
24) R. Archibald, F. Bao, Y. Cao, and H. Sun, "Numerical analysis for convergence of a sample-wise backpropagation method for training stochastic neural networks." *SIAM Journal on Numerical Analysis*, 62(2) 593-621 (2024). https://doi.org/10.1137/22M1523765
25) H.A. Kazem, M.T. Chaichan, H.S. Abd, A.H. Al-Waeli, M.T. Mahdi, H.H. Fadhil, I.I. Mohd, and A.A. Khadom, "Performance evaluation of solar photovoltaic/thermal system performance: An experimental and artificial neural network approach," *Case Studies in Thermal Engineering*, 104860 (2024). https://doi.org/10.1016/j.csite.2024.104860
26) M.A. Essa, A. M. Rashad, and A.Y. Hatata, "A novel FFNN-AHO hybrid predictive model for enhancing the performance of jet-cooled PVT system." *Indonesian Journal of Electrical Engineering and Computer Science*, 2024 (2) 711-725 (2024). https://doi.org/10.11591/ijeecs.v34.i2.pp711-725
27) X. Zhang, and C.A. Liu, "Model averaging prediction by K-fold cross-validation." *Journal of Econometrics*, 235(1) 280-301 (2023). https://doi.org/10.1016/j.jeconom.2022.04.007
28) A.R. Kamel, and M.R. Abonazel, "A simple introduction to regression modeling using R." *Computational Journal of Mathematical and Statistical Sciences*, 2(1) 52-79 (2023). https://doi.org/10.21608/cjmss.2023.189834.1002
29) B. Yaniktepe, O. Kara, and C. Ozalp, "Estimation of the solar radiation model using measured data of Osmaniye," In *RAD Conference Proceedings*-Turkey, 2, 195-197 (2017). https://www.rad-proceedings.org/home.php (Accessed 11 November 2024)
30) S. Ghimire, T. Nguyen-Huy, R. Prasad, R.C. Deo, D. Casillas-Pérez, S. Salcedo-Sanz, and B. Bhandari, "Hybrid convolutional neural network-multilayer perceptron model for solar radiation prediction.: *Cognitive Computation*, 15(2) 645-671 (2023). https://doi.org/10.1007/s12559-022-10070-y
31) O. Büyükalaca, H.M. Kılıç, U. Olmuş, Y.E. Güzelel, and K.N. Çerçi, "Numerical investigation and ANN modeling of performance for hexagonal boron Nitride-water nanofluid PVT collectors". *Thermal Science and Engineering Progress*, 43 101997 (2023). https://doi.org/10.1016/j.tsep.2023.101997
32) M. Abd Elaziz, S. Senthilraja, M.E. Zayed, A.H. Elsheikh, R.R. Mostafa, and S. Lu, "A new random vector functional link integrated with mayfly optimization algorithm for performance prediction of solar photovoltaic thermal collector combined with electrolytic hydrogen production system," *Applied Thermal Engineering*, 193 117055 (2021). https://doi.org/10.1016/j.applthermaleng.2021.117055
33) A.H. Al-Waeli, K. Sopian, J.H. Yousif, H.A. Kazem, J. Boland, and M.T. Chaichan, "Artificial neural network modelling and analysis of photovoltaic/thermal system based on the experimental study," *Energy Conversion and Management*, 186 368-379 (2019). https://doi.org/10.1016/j.enconman.2019.02.066
34) I.M. Mfetoum, S.K. Ngoh, R.J.J. Molu, B.F. Nde Kenfack, R. Onguene, S.R.D. Naoussi, J.G. Tamba, M. Bajaj, and M. Berhanu, "A multilayer perceptron neural network approach for optimizing solar irradiance forecasting in Central Africa with meteorological insights." *Scientific Reports*, 14(1) 3572 (2024). https://doi.org/10.1038/s41598-024-54181-y
35) A.H. Al-Waeli, H. A. Kazem, J.H. Yousif, M.T. Chaichan, and K. Sopian, "Mathematical and neural network modeling for predicting and analyzing of nanofluid-nano PCM photovoltaic thermal systems performance," *Renewable Energy*, 145 963-980 (2020). https://doi.org/10.1016/j.renene.2019.06.099

36) H. Gharaee, M. Erfanimatin, and A.M. Bahman, “Machine learning development to predict the electrical efficiency of photovoltaic-thermal (PVT) collector systems.” *Energy Conversion and Management*, 315 118808 (2024). https://doi.org/10.1016/j.tsep.2023.101997
37) I. Kayri, “The effects of coolant mass flow rate and atmospheric indicators in a PV/T system with experimental and ANN’s models.” *Sustainable Energy, Grids and Networks*, 36 101189 (2023). https://doi.org/10.1016/j.segan.2023.101189